Supplementary Materials for

Molecular Trap Engineering Enables Superior High-Temperature Charge-Discharge Efficiency in a Polymer Blend with Densely Packed Molecular Chains

Qiyan Zhang, *[ab] Juntian Zhuo, [ab] Wugang Liao, [ab] Shuangwu Huang, *[ab] Shuxiang Dong [c]

a. *State Key Laboratory of Radio Frequency Heterogeneous Integration, Shenzhen University, Shenzhen 518060, China*

b. *College of Electronics and Information Engineering, Institute of Microelectronics (IME), Shenzhen University, Shenzhen 518060, China*

c. *Institute for Advanced Study, Shenzhen University, Shenzhen, 518061, China*

†Correspondence: zhangqy@szu.edu.cn, mark_huang@szu.edu.cn

This PDF file includes:

Experiment and Figures. S1 to S9.

Experiment

Materials. PEI (Ultem 1000) and TPI (Matrimid 5218) were provided by PolyK Technologies, United States. [6,6]-phenyl-C61-butyric acid methyl ester (PC61BM), 1,4,5,8-naphthalenetetracarboxylic dianhydride (NTCDA), and N-Methyl pyrrolidone (NMP) were purchased from Aladdin Chemistry Co. Ltd., China. All chemicals used were of analytical grade and were employed without further purification.

Preparation of polymer blend-based all-organic composites. The composite films were prepared using the solution casting method. First, a blend solution was prepared by dissolving TPI powder and PEI pellets in NMP at a weight ratio of 50%/50%. This mixture was stirred for 5 hours at 70℃ to obtain a clear and homogeneous solution. Next, the organic molecular semiconductors (PC61BM or NTCDA) were dissolved in NMP at a concentration of 4 mg/ml. The NMP solution of the organic molecular semiconductors was then added to the blend solution in the desired proportion, and the resulting mixture was stirred for an additional 8 hours at 70℃. The solution was drop-casted on a clean glass slide and placed in a drying oven at 80 ℃ for 12 hours to remove the solvent. It was then heated sequentially to 120 ℃ for 2 hours, 150 ℃ for 2 hours, and 180 ℃ for 5 hours to slowly remove the solvent, thereby preventing defects such as bubbles that could result from rapid solvent evaporation. The films were further dried under vacuum at 200 °C for 12 hours to completely eliminate any residual solvent. The cast film was then peeled off the glass substrate in deionized water and subsequently dried at 200 ℃ in a vacuum oven for an additional 12 hours to obtain free-standing films.

Characterizations. The typical thickness of the films used for electrical characterizations is approximately 10 μm, as measured

by a Millimar C1200M compact length measuring instrument. Gold electrodes with a diameter of 6 mm and thicknesses of 60 nm were sputtered onto both sides of the polymer films for all the electrical measurements. Thermally Stimulated Depolarization Current (TSDC) was measured using a PK-SPIV17 measurement system (PolyK Technologies, United States). Samples were first polarized at 260°C for 20 minutes under an electric field of 50 MV/m. After polarization, the temperature was rapidly cooled down to 100°C at a rate of 20°C/min with the applied electric field, and then the sample was short-circuited for 5 minutes. Finally, the temperature was increased to 260°C at a rate of 3°C/min and the current was recorded using a Keithley 6517B electrometer. Conduction currents were measured under various electric fields using a Keithley 6517B pA meter and a Trek 610E amplifier as the DC voltage source. The breakdown strengths at 150 ℃ and 200 ℃ were measured using a high-voltage amplifier system (Trek 610E, United States). Temperature control was achieved with a digital hot plate equipped with a thermocouple. Breakdown strengths were determined by applying a two-parameter Weibull statistical analysis on more than 10 samples. Dielectric spectra were obtained over a broad temperature range from 25 ℃ to 200 ℃ and a frequency range from 100 Hz to 1 MHz using a Keysight E4980AL LCR meter. Measurements were conducted in a Sun Systems environmental chamber equipped with a liquid nitrogen cooling system. The electric displacement-electric field (*D*-*E*) loops of the films at different temperatures were measured using a modified Sawyer-Tower circuit with a Trek 610E high-voltage amplifier system under a unipolar triangle voltage at a frequency of 100 Hz. All *D*-*E* loop measurements were conducted with the sample immersed in insulating silicone oil, with temperature control provided by a digital hot plate equipped with a thermocouple. Cyclic charge–discharge tests were performed using a PK-CPR1502 test system (PolyK Technologies, United States).

DFT calculations. DFT is based on the first-principles calculation and the wave functions of calculated molecules are determined according to the solution of basic Schrodinger's equation. DFT calculations in this work were performed using the Gaussian 16 program package, B3LYP functional with 6-31G(d,p) basis set.[1,2] In this work, the highest occupied molecular orbital (HOMO) energy levels, and lowest unoccupied molecular orbital (LUMO) energy levels for TPI units, PEI units, NTCDA, and PC61BM were calculated using density functional theory (DFT) with the B3LYP functional and a 6-31G(d,p) basis set. Additionally, the spatial distribution of electrostatic potential for NTCDA and PC61BM was also determined.

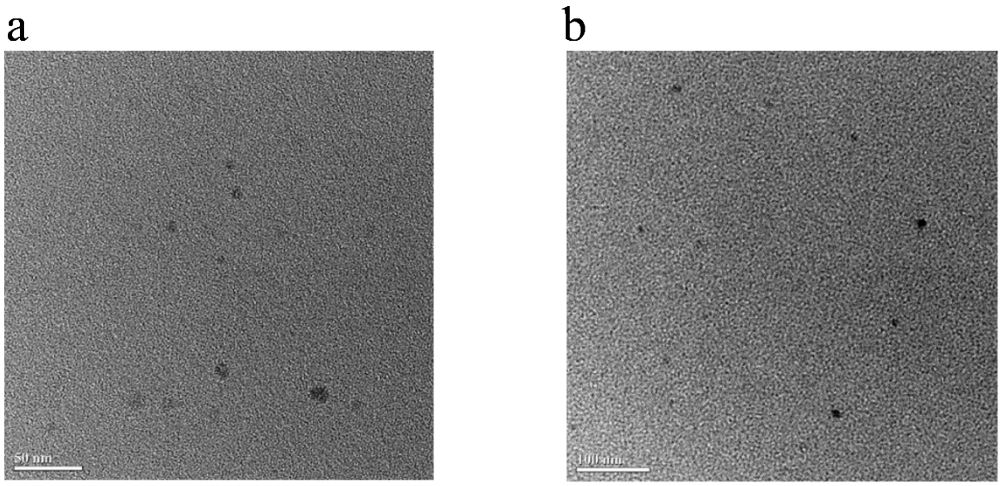

Figure S1. TEM images of (a) TPI/PEI/PC61BM (0.75 wt.% PC61BM) and (b) TPI/PEI/NTCDA (2.0 wt.% NTCDA) composites.

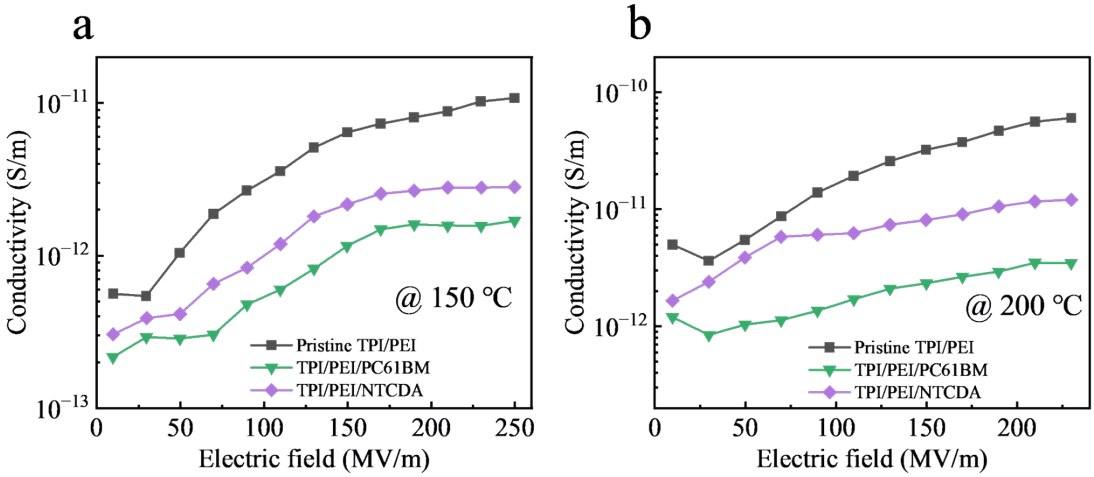

Figure S2. Electric field-dependent conductivity of pristine TPI/PEI blend, TPI/PEI/PC61BM (0.75 wt.% PC61BM) and TPI/PEI/NTCDA (2.0 wt.% NTCDA) composites at (a) 150 ℃ and (b) 200 ℃.

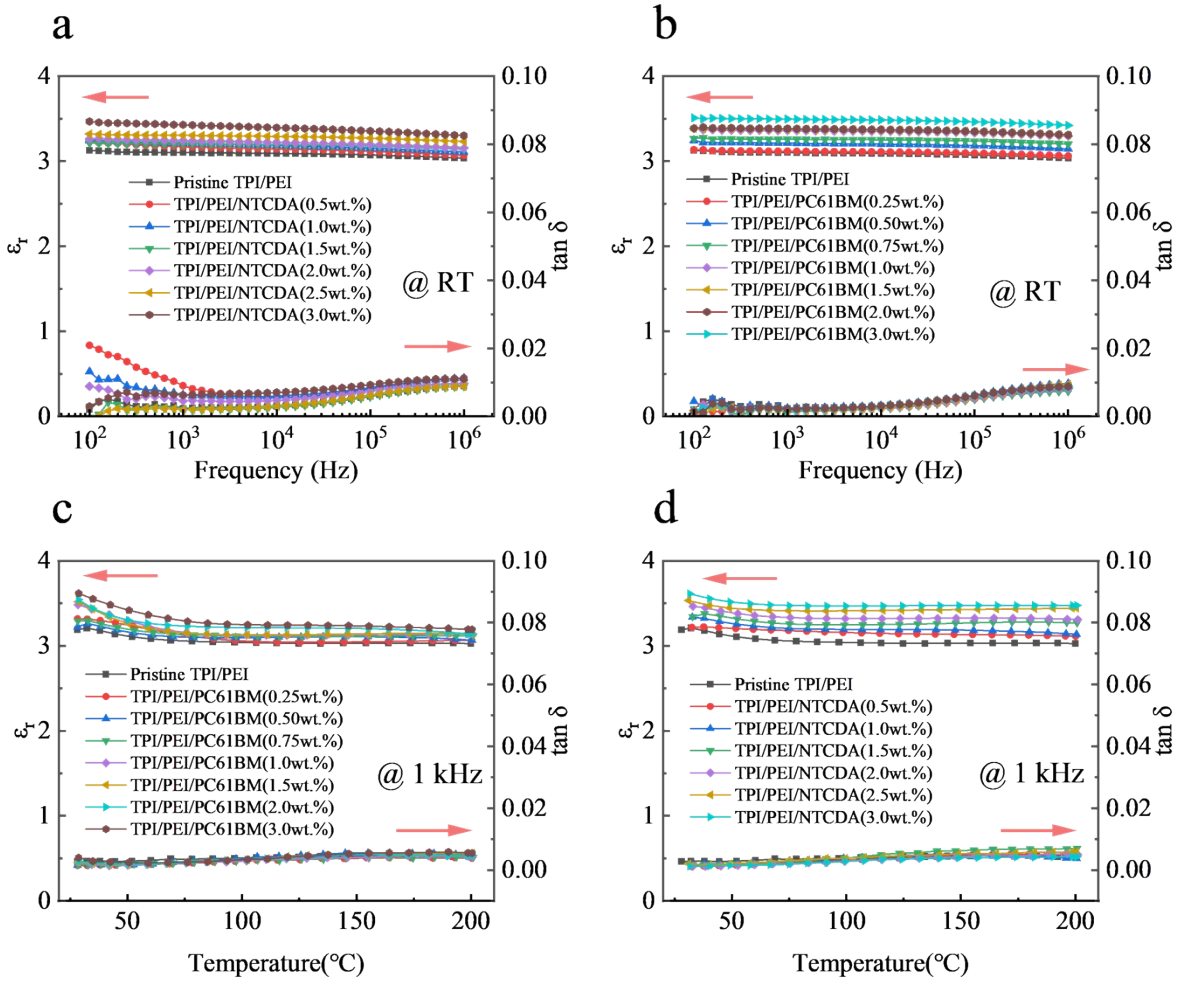

Figure S3. Frequency-dependent dielectric constants and dissipation factors of (a) TPI/PEI/NTCDA and (b) TPI/PEI/PC61BM composites at room temperature. Temperature-dependent dielectric constants and dissipation factors at 1 kHz for (c) TPI/PEI/PC61BM and (d) TPI/PEI/NTCDA composites.

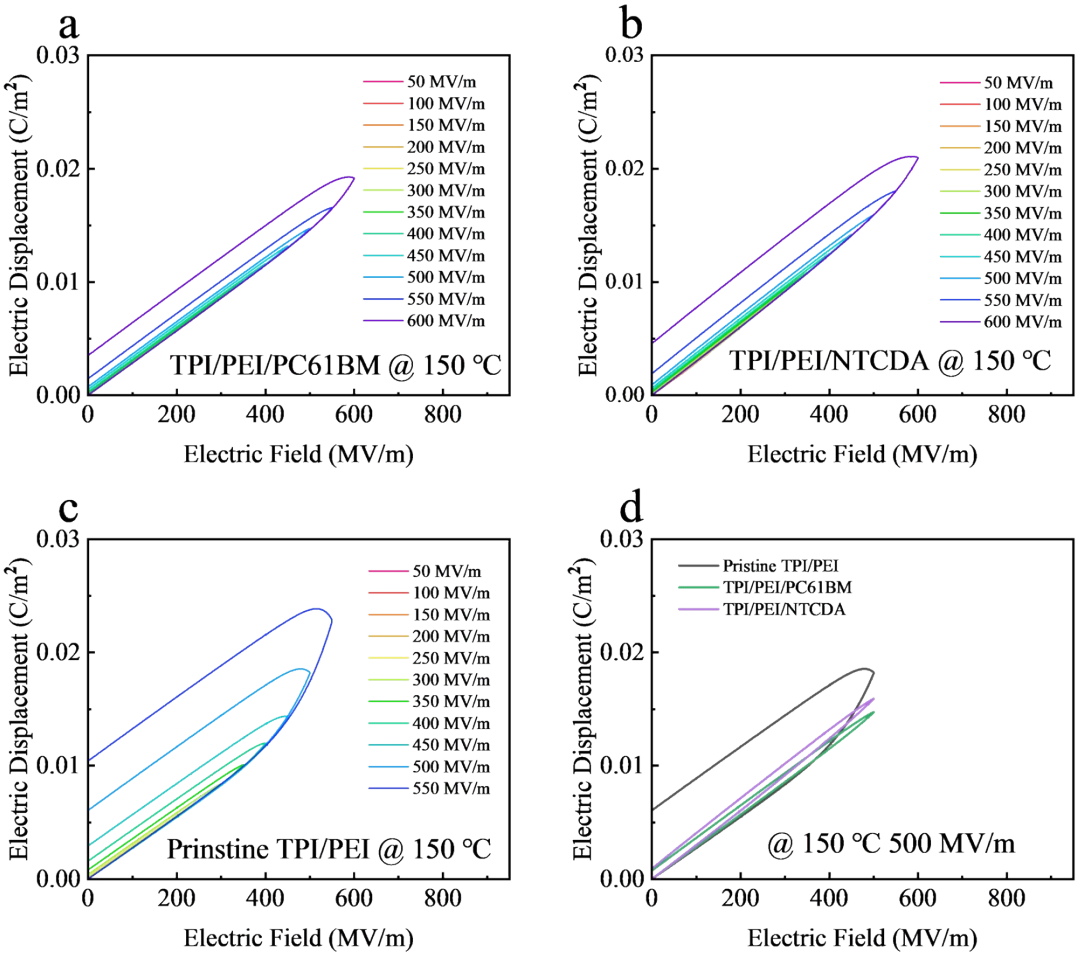

Figure S4. Unipolar *D-E* loops of (a) TPI/PEI/PC61BM (0.75 wt.% PC61BM), (b) TPI/PEI/NTCDA (2.0 wt.% NTCDA), and (c) pristine TPI/PEI blend measured at 150 °C. (d) Comparison of pristine TPI/PEI blend, TPI/PEI/PC61BM (0.75 wt.% PC61BM), and TPI/PEI/NTCDA (2.0 wt.% NTCDA) measured at 150 °C and 500MV/m.

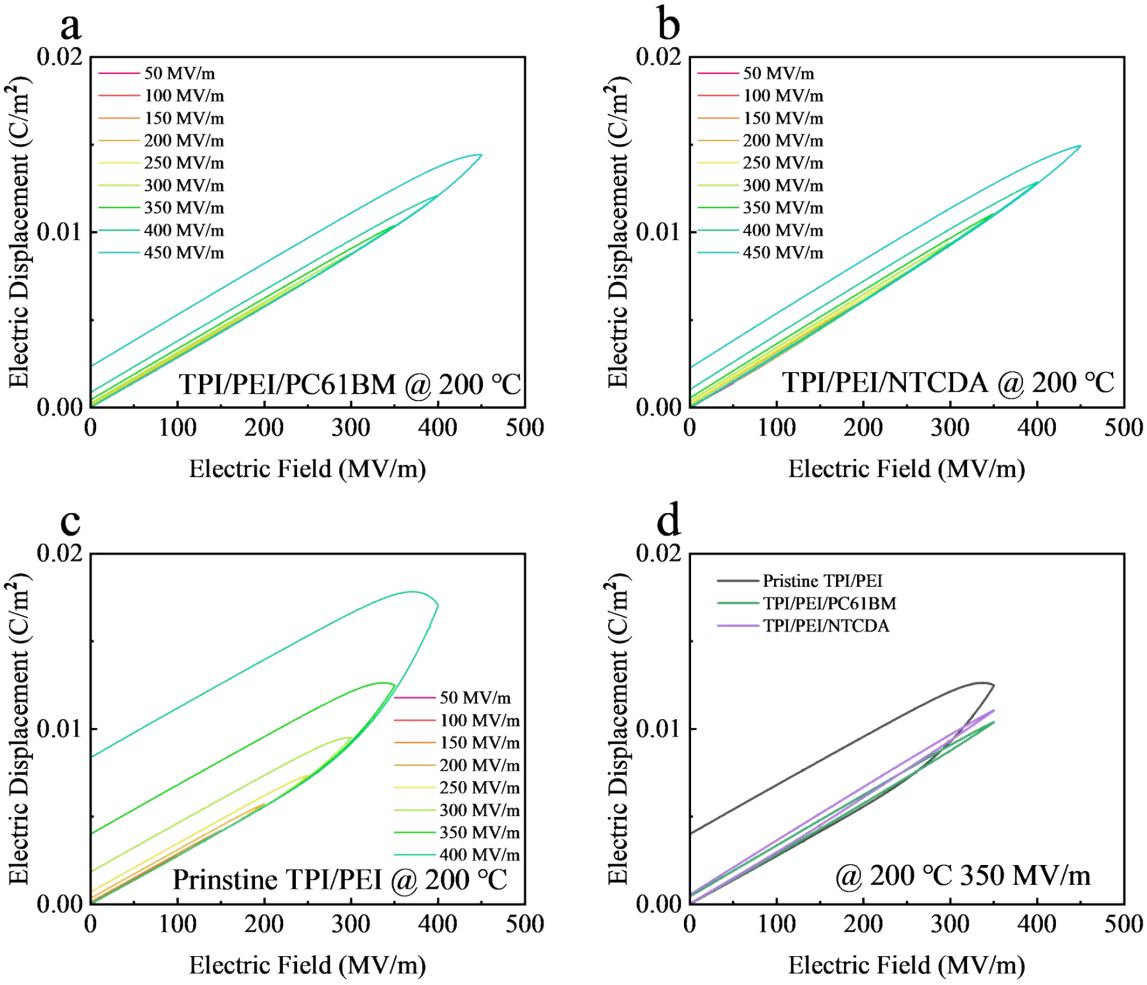

Figure S5. Unipolar *D-E* loops of (a) TPI/PEI/PC61BM (0.75 wt.% PC61BM), (b) TPI/PEI/NTCDA (2.0 wt.% NTCDA), and (c) pristine TPI/PEI blend measured at 200 °C. (d) Comparison of pristine TPI/PEI blend, TPI/PEI/PC61BM (0.75 wt.% PC61BM), and TPI/PEI/NTCDA (2.0 wt.% NTCDA) measured at 200 °C and 350 MV/m.

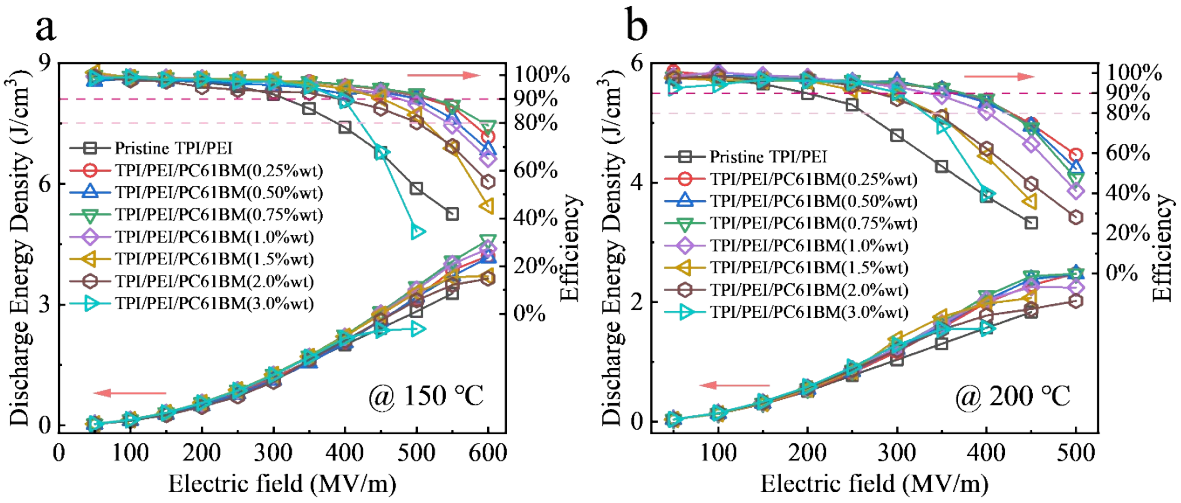

Figure S6. Discharged energy density and charge-discharge efficiency of TPI/PEI/PC61BM composites at (a) 150 °C and (b) 200 °C.

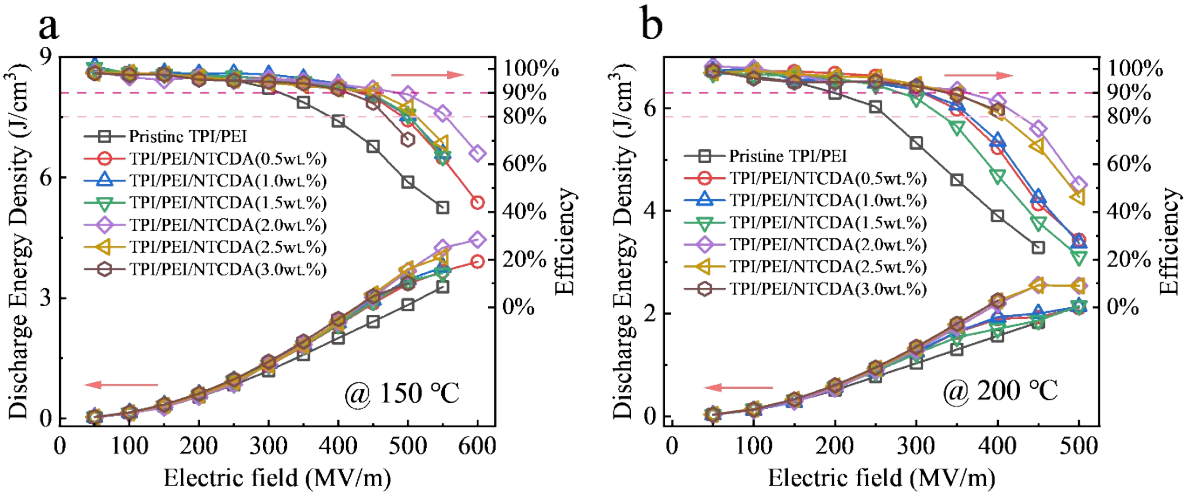

Figure S7. Discharged energy density and charge-discharge efficiency of TPI/PEI/NTCDA composites at (a) 150 °C and (b) 200 °C.

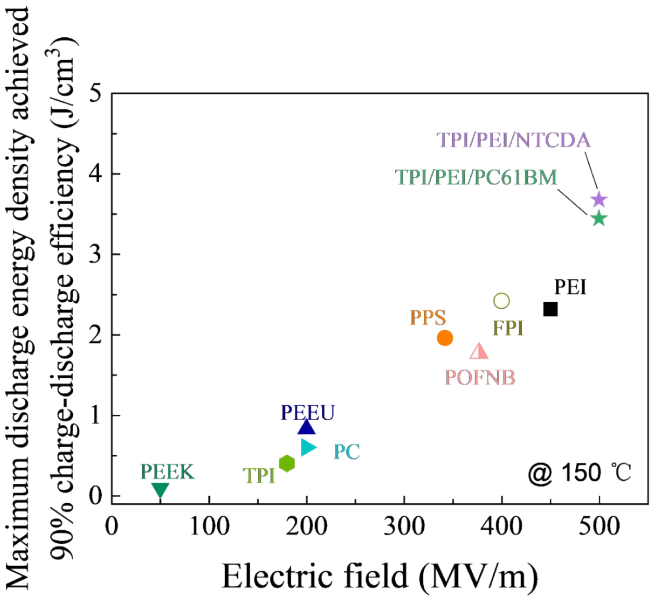

Figure S8. Comparison of discharged energy density at 150 °C and above 90 % efficiency between this work and other dielectric polymers (PEI[3], PPS[4], PEEU[5], PC[6], PEEK[6], TPI[7], FPI[8] and POFNB[9]). The comparisons are based on results obtained at a frequency of 100 Hz for the frequency dependence of charge–discharge efficiency.

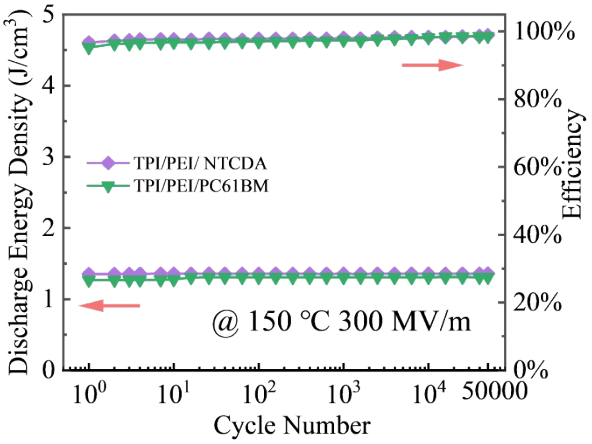

Figure S9. Cyclic performance of TPI/PEI/PC61BM (0.75 wt.% PC61BM) and TPI/PEI/NTCDA (2.0 wt.% NTCDA) at 150 °C and 300 MV/m electric field.

Reference:

1 T. Yanai, D. P. Tew and N. C. Handy, *Chemical Physics Letters*, 2004, **393**, 51–57.

2 E. K. U. Gross and W. Kohn, *Phys. Rev. Lett.*, 1985, **55**, 2850–2852.

3 B. Zhang, X. Chen, Z. Pan, P. Liu, M. Mao, K. Song, Z. Mao, R. Sun, D. Wang and S. Zhang, *Adv Funct Materials*, 2023, **33**, 2210050.

4 M. Lin, J. Zhuo, S. Huang, Q. Zhang and Q. M. Zhang, *Chemical Engineering Journal*, 2024, **498**, 155586.

5 T. Zhang, X. Chen, Y. Thakur, B. Lu, Q. Zhang, J. Runt and Q. M. Zhang, *Sci. Adv.*, 2020, **6**, eaax6622.

6 J. Chen, Y. Zhou, X. Huang, C. Yu, D. Han, A. Wang, Y. Zhu, K. Shi, Q. Kang, P. Li, P. Jiang, X. Qian, H. Bao, S. Li, G. Wu, X. Zhu and Q. Wang, *Nature*, 2023, **615**, 62–66.

7 Q. Zhang, X. Chen, B. Zhang, T. Zhang, W. Lu, Z. Chen, Z. Liu, S. H. Kim, B. Donovan, R. J. Warzoha, E. D. Gomez, J. Bernholc and Q. M. Zhang, *Matter*, 2021, **4**, 2448–2459.

8 M. Liu, J. Song, H. Qin, S. Qin, Y. Zhang, W. Xia, C. Xiong and F. Liu, *Adv. Funct. Mater.*, 2024, **34**, 2313258.

9 A. A. Deshmukh, C. Wu, O. Yassin, A. Mishra, L. Chen, A. Alamri, Z. Li, J. Zhou, Z. Mutlu, M. Sotzing, P. Rajak, S. Shukla, J. Vellek, M. A. Baferani, M. Cakmak, P. Vashishta, R. Ramprasad, Y. Cao and G. Sotzing, *Energy Environ. Sci.*, 2022, **15**, 1307–1314.